THE STRUCTURAL DESIGN OF TALL AND SPECIAL BUILDINGS
*Struct. Design Tall Spec. Build.* **15**, 325–338 (2006)
Published online in Wiley Interscience (www.interscience.wiley.com). **DOI**: 10.1002/tal.298

# RESONANT BEHAVIOUR OF BASE-ISOLATED HIGH-RISE BUILDINGS UNDER LONG-PERIOD GROUND MOTIONS

T. ARIGA, Y. KANNO AND I. TAKEWAKI*
*Department of Urban and Environmental Engineering, Graduate School of Engineering, Kyoto University, Kyoto, Japan*

SUMMARY

The resonant behaviour of base-isolated high-rise buildings under long-period ground motions is investigated. The long-period ground motions are known to be induced by surface waves. While the acceleration amplitude of such long-period ground motion is small, the velocity amplitude is fairly large. It is expected that high-rise buildings and base-isolated buildings with long fundamental natural periods are greatly influenced by these long-period ground motions. Especially base-isolated high-rise buildings with friction-type bearings may have remarkable mechanical characteristics unfavourable for these long-period ground motions. The purpose of this paper is to reveal that the long-period ground motions recorded in Japan have the intensity to make base-isolated high-rise buildings in resonance with long-period components and that careful treatment is inevitable in the structural design of these base-isolated high-rise buildings. It is pointed out that the friction-type bearings are effective in general in avoiding the resonance with ground motions with a narrow-range frequency characteristic, but are dangerous for ground motions with a wide-range frequency characteristic in the long period range. Copyright © 2006 John Wiley & Sons, Ltd.

## 1. INTRODUCTION

It is commonly recognized (e.g., see Naeim and Kelly, 1999) that base-isolation (BI) systems are very useful in reducing the earthquake response of buildings and are being installed in many buildings and facilities after the Hyogo-ken Nanbu earthquake (1995). This observation is based on the fact that BI systems are effective for ground motions including mainly high-frequency components. In fact, most of the ground motions recorded in the United States include high-frequency components in general and long-period ground motions (Kamae *et al*., 2004) have never been discussed except a few cases, e.g. Landers in 1992, Northridge in 1995, (Heaton *et al*., 1995; Hall *et al*., 1995; Janjid and Kelly, 2001). Even in these cases, the frequency range of the long-period components, so-called pulse waves, is rather short (2–3 s) compared to those (5–10 s) discussed in Japan. Recently not a few base-isolated high-rise building structures have been under construction in Japan. Most of these base-isolated high-rise building structures contain friction-type BI systems. Friction-type BI systems are very useful in lengthening the equivalent natural period of BI systems and in avoiding resonance with ground motions including rather high-frequency components. However, these characteristics should be reconsidered in the case where the design ground motions contain long-period components in the period range comparable with the equivalent natural period of BI systems (Kobori, 2004).

The purpose of this paper is to reveal that the long-period ground motions recorded in Japan have the intensity to make base-isolated high-rise buildings in near resonance with the long-period com-

*Correspondence to: I. Takewaki, Department of Urban and Environmental Engineering, Graduate School of Engineering, Kyoto University, Sakyo, Kyoto, 606-8501, Japan. E-mail: takewaki@archi.kyoto-u.ac.jp

ponents and that careful treatment is absolutely necessary in the structural design of these base-isolated high-rise buildings.

## 2. BASE-ISOLATED HIGH-RISE BUILDINGS

Consider an $N$-storey shear building model, as shown in Figure 1, supported by a BI system. Let $m_i,k_i,c_i$ denote the mass of the $(i + 1)$-th floor, the stiffness of the $i$-th story and the corresponding damping coefficient, respectively. It is assumed here that the BI system consists of linear rubber bearings, friction-type bearings and additional viscous damper systems as shown in Figure 2 and can be modelled by a normal bilinear hysteretic spring of the restoring force $f_0(u_1)$ as shown in Figure 3 and a linear viscous damper. This modelling results from the linear elastic constitutive law of linear rubber bearings and the elastic perfectly plastic constitutive law of friction-type bearings. It should be noted that $f_0(u_1)$ is path-dependent. The horizontal initial stiffness of the BI system and the damping coefficient of the additional viscous damper system are denoted by $k_0,c_0$, respectively. This model is subjected to a horizontal acceleration $\ddot{u}_g(t)$ at the ground surface.

Let $u_i$ denote the horizontal displacement of the $(i + 1)$-th floor. The equations of motion of this BI building may be expressed as

$$\mathbf{M}\ddot{\mathbf{u}} + \mathbf{C}\dot{\mathbf{u}} + \mathbf{F}(\mathbf{u}) = -\mathbf{M}\mathbf{1}\ddot{u}_g \tag{1}$$

where $\mathbf{u} = \{u_0\ u_1\ \ldots\ u_N\}^T$ and $\mathbf{F}(\mathbf{u}) = \mathbf{K}_B\mathbf{u} + \mathbf{F}_I(u_1)$. $\mathbf{M},\mathbf{K}_B,\mathbf{F}_I(u_1),\mathbf{C},\mathbf{1}$ are the following matrices and a vector:

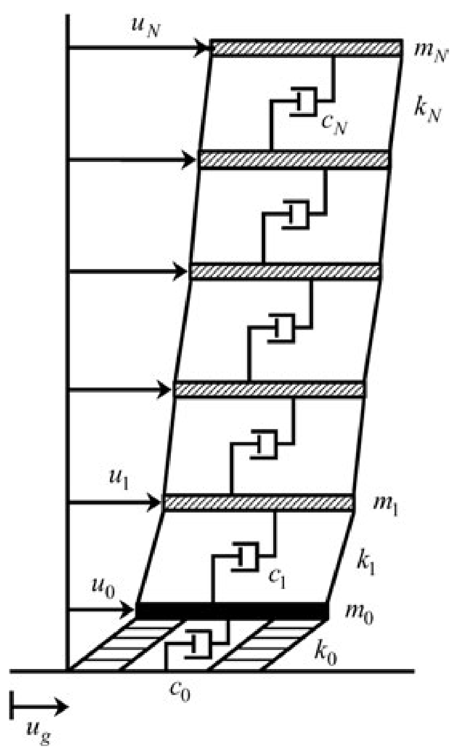


Figure 1. $N$-storey shear building model supported by a BI system

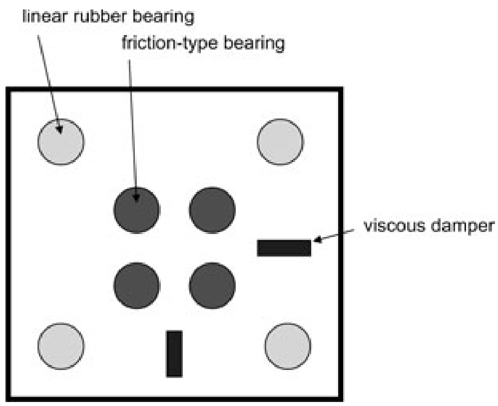


Figure 2. BI system consisting of linear rubber bearings, friction-type bearings and additional viscous dampers

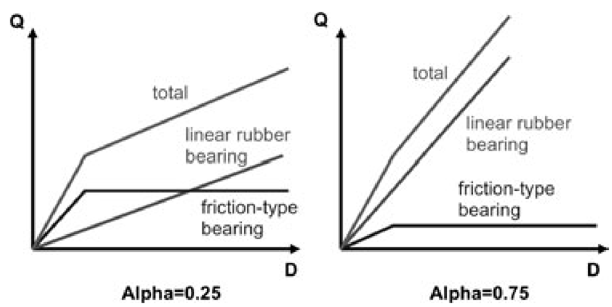


Figure 3. Restoring force characteristics of linear rubber bearing and friction-type bearing

$$\mathbf{M} = \mathrm{diag}(m_0\ m_1 \cdots m_N) \tag{2a}$$

$$\mathbf{K}_B = \begin{bmatrix} k_1 & -k_1 & & \mathbf{0} \\ -k_1 & \ddots & \ddots & \\ & \ddots & k_{N-1}+k_N & -k_N \\ \mathbf{0} & & -k_N & k_N \end{bmatrix} \tag{2b}$$

$$\mathbf{F}_I(u_1) = \mathrm{diag}(f_0(u_1)\ 0 \cdots 0) \tag{2c}$$

$$\mathbf{C} = \begin{bmatrix} c_0+c_1 & -c_1 & & \mathbf{0} \\ -c_1 & \ddots & \ddots & \\ & \ddots & c_{N-1}+c_N & -c_N \\ \mathbf{0} & & -c_N & c_N \end{bmatrix} \tag{2d}$$

$$\mathbf{1} = \{1\,1 \cdots 1\}^T \tag{2e}$$



**DOI**: 10.1002/tal

## 3. NUMERICAL EXAMPLES

### *3.1 Building data and input ground motions*

Originally BI systems were applied to rather low-rise buildings. However, BI systems are being installed in mid-rise or high-rise buildings especially in Japan. In order to clarify the earthquake response characteristics of these mid-rise or high-rise buildings with BI systems, numerical examples for 10-storey shear building models with BI systems are presented here. Ten-storey buildings are not so high, but their properties, especially the natural period characteristics, are based on the realistic data used in Japan.

The floor masses are $m_i = 3{\cdot}20 \times 10^5$ (kg) ($i = 1, \ldots, 10$) and $m_0 = 9{\cdot}60 \times 10^5$ (kg). The storey stiffnesses of the building are determined so that the 10-storey shear building model with fixed base has a fundamental natural period of 1·0 (s) and the lowest eigenmode of the model with fixed base is straight. This treatment is based on the inverse problem approach (Nakamura and Yamane, 1986). The initial stiffness $k_0$ and damping coefficient $c_0$ of the BI system have been determined so that the initial natural period of the base-isolated rigid building model ($k_i \to \infty$ ($i = 1, \ldots, 10$)) is 4·0 (s) and the initial damping ratio of the base-isolated rigid building model is 0·02 or 0·10.

Four cases are investigated. The ratio of the total stiffness of the linear rubber bearings to the total initial stiffness of the BI system (sum of the total stiffness of linear rubber bearings and that of friction-type bearings) is denoted by $\alpha$. This coefficient $\alpha$ is also the ratio of the second horizontal stiffness to the initial horizontal stiffness in the normal bilinear hysteretic characteristic in the BI system. The first case is the case ($\alpha = 1{\cdot}0$) where there is no friction-type rubber bearing and all the stiffness $k_0$ is the stiffness of the linear rubber bearings. The second, third and fourth cases correspond to $\alpha =$ 0·75, 0·50 and 0·25, respectively. The dynamic friction coefficient of the friction-type bearing systems is assumed to be 0·024. The static friction coefficient is larger than the dynamic one but this phenomenon is disregarded in the present analysis. It is assumed that half of the building weight is supported by linear rubber bearings and the other half by friction-type rubber bearings in the case of $\alpha =$ 0·75, 0·50, 0·25. The limit shear force in the friction-type rubber bearings can be computed by multiplication of half the total weight of the building by the friction coefficient 0·024 in the case of $\alpha =$ 0·75, 0·50, 0·25. The initial horizontal stiffness of friction-type rubber bearings can be expressed by $(1 - \alpha)k_0$. It has been ascertained that the mean vertical normal stress in linear rubber bearings and friction-type rubber bearings is around 10 (N/mm$^2$).

The initial value of the fundamental natural period of the BI building model is 4·08 (s). The damping matrix of the building is assumed to be proportional to the stiffness matrix and the lowest-mode damping ratio of the building with fixed-base is 0·05. It should be noted that a rather long fundamental natural period of the BI building model is assumed here to disclose the resonant characteristic of the BI building model. However, a similar situation can occur even in models of higher buildings.

Four ground motions are used as input motions: El Centro NS (Imperial Valley 1940), OSA NS (simulated Nankai earthquake by Kamae *et al*., 2004), Tomakomai EW (Tokachi-Oki, 2003) and a simulated motion compatible with the response spectrum (damping ratio 0·05) of level 2 for safety check in the new Japanese Earthquake-resistant Design Code (2000). The acceleration response spectrum $S_A$ (m/s$^2$) (damping ratio 0·05) in the new Japanese Earthquake-resistant Design Code (2000) is given by

$$S_A = 3{\cdot}2 + 30{\cdot}0T \qquad (T < 0{\cdot}16\,\text{s}) \tag{3a}$$

$$S_A = 8{\cdot}0 \qquad (0{\cdot}16\,\text{s} \le T \le 0{\cdot}64\,\text{s}) \tag{3b}$$

$$S_A = 5{\cdot}12/T \qquad (0{\cdot}64\,\text{s} < T) \tag{3c}$$



**DOI**: 10.1002/tal

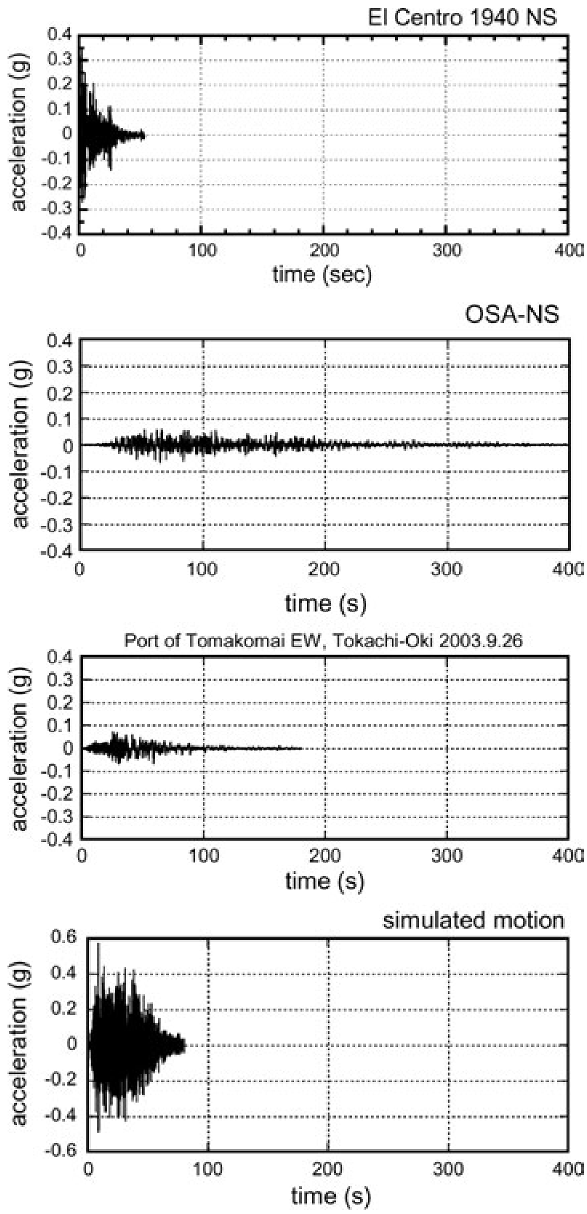


Figure 4. Acceleration records of El Centro NS (Imperial Valley, 1940), OSA NS (simulated Nankai Earthquake by Kamae *et al.*, 2004), Tomakomai EW (Tokachi-Oki, 2003) and a simulated motion compatible with the response spectrum of level 2 in the new Japanese Earthquake-resistant Design Code (2000)

The acceleration records of these motions are shown in Figure 4 and the velocity response spectra of these motions for damping ratio 0·05 are shown in Figure 5. The velocity record of Tomakomai EW is shown in Figure 6 for reference. The compatibility of the velocity response spectrum of the simulated motion with the target spectrum is shown in Figure 7.



**DOI**: 10.1002/tal

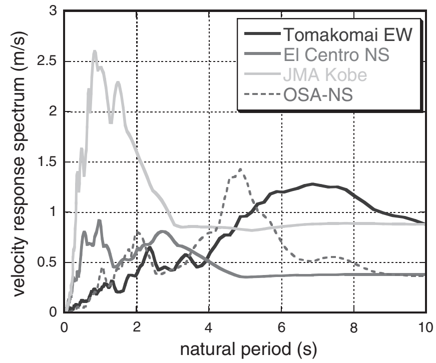


Figure 5. Velocity response spectra of four motions considered for damping ratio 0·05

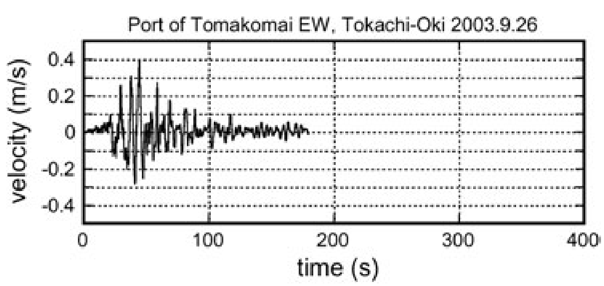


Figure 6. Velocity record of Tomakomai EW (Tokachi-Oki, 2003)

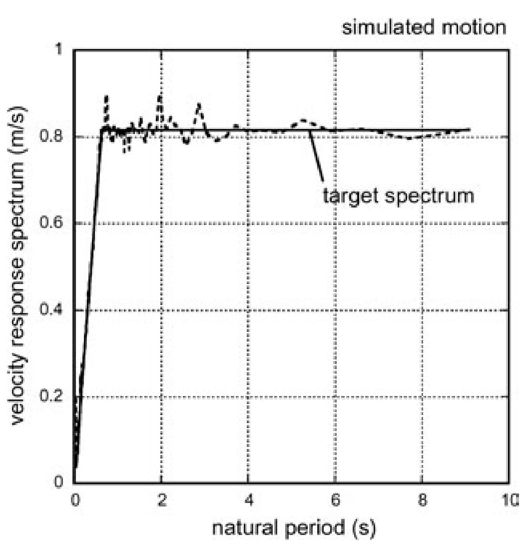


Figure 7. Compatibility of the velocity response spectrum of simulated motion with target spectrum (damping ratio 0·05)



**DOI**: 10.1002/tal

### *3.2 Response characteristics*

First of all, the damping ratio of the additional viscous damper system in the BI system is assumed to be 0·02. Figure 8 shows the restoring force characteristics in the BI system under four ground motions in the case of $\alpha = 1{\cdot}0$. The case of $\alpha = 1{\cdot}0$ corresponds to the BI system without friction-type bearings and the restoring force characteristics of the BI system are linear elastic. It can be observed that the maximum drift under El Centro NS is almost one-third of that under OSA NS, Tomakomai EW and simulated motion.

Figure 9 illustrates the restoring force characteristics in the BI system under four ground motions in the case of $\alpha = 0{\cdot}75$. It can be observed that the restoring force characteristics in the BI system under OSA NS and Tomakomai EW exhibit hysteretic behaviours but the maximum drifts are similar to those in the case of $\alpha = 1{\cdot}0$. On the other hand, the maximum drift under the simulated motion is almost two-thirds of that in the case of $\alpha = 1{\cdot}0$. This may result from the increase in damping and the constant characteristics of the velocity response spectrum of the simulated motion.

Figure 10 shows the restoring force characteristics in the BI system under four ground motions in the case of $\alpha = 0{\cdot}50$. It can be observed that the restoring force characteristics in the BI system under

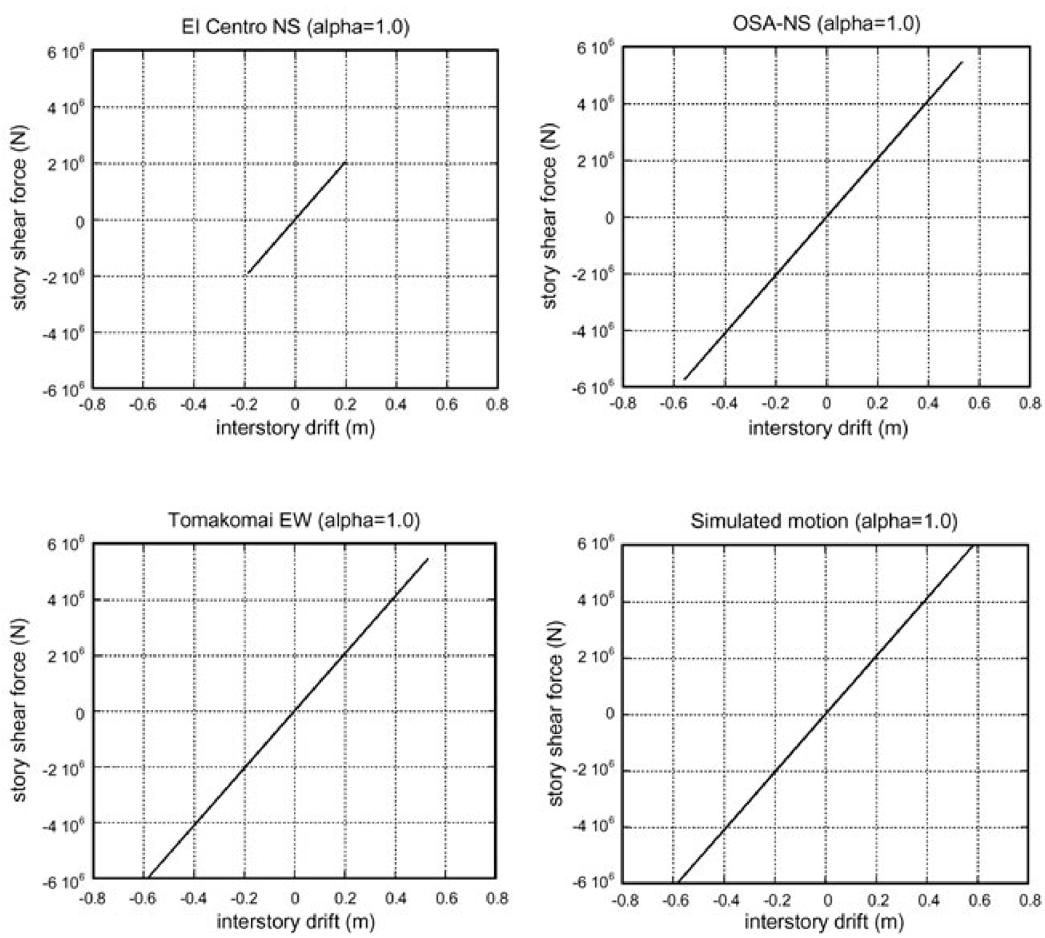


Figure 8. Restoring force characteristics in the BI system under four ground motions in the case of $\alpha = 1{\cdot}0$



**DOI**: 10.1002/tal

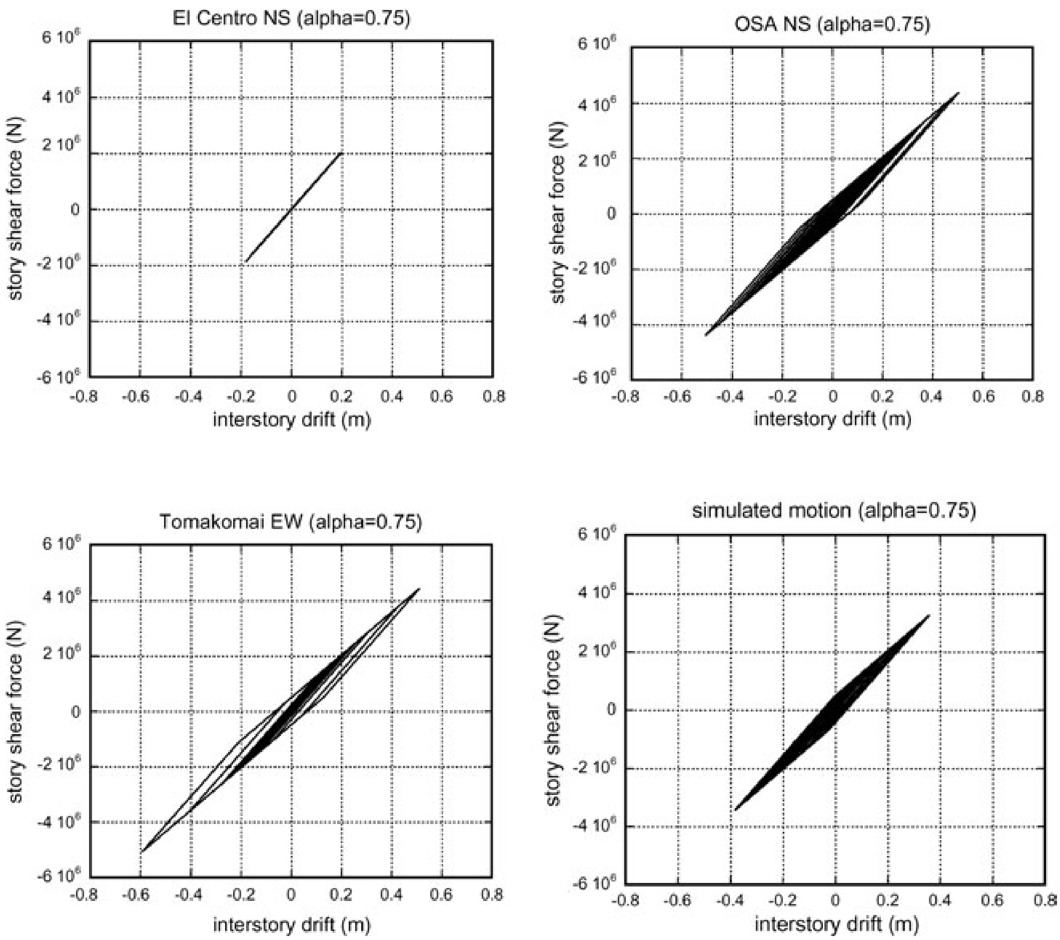


Figure 9. Restoring force characteristics in the BI system under four ground motions in the case of $\alpha = 0{\cdot}75$

four ground motions exhibit hysteretic behaviours and the maximum drift under Tomakomai EW is larger than that in the case of $\alpha = 1{\cdot}00$, $0{\cdot}75$.

Figure 11 indicates the restoring force characteristics in the BI system under four ground motions in the case of $\alpha = 0{\cdot}25$. It can be observed that, while the maximum interstorey drift in the BI system under OSA NS is smaller than that in the case of $\alpha = 1{\cdot}00$, $0{\cdot}75$, $0{\cdot}50$, the maximum interstorey drift under Tomakomai EW is much larger than that in the case of $\alpha = 1{\cdot}00$, $0{\cdot}75$. It can be expected that a nearly resonant behaviour occurs in this case. The equivalent damping ratio in this case is about 0·14, which has been obtained by using the secant stiffness in the computation of the equivalent natural period (7·25 s) and equating the dissipated energy by the hysteretic behaviour with that in the corresponding viscous damping model. Figure 12 shows the velocity response spectra for various damping ratios for Tomakomai EW. While the fundamental natural period and the approximate lowest-mode damping ratio in the case of $\alpha = 1{\cdot}0$ are 4·08 s and 0·02, respectively, those in the case of $\alpha = 0{\cdot}25$ for Tomakomai EW are 7·25 s and 0·14, respectively. It can be observed from Figure 12 that the velocity response spectra for these two cases are almost the same. However, it should be kept in mind that the displacement response spectrum is derived by dividing the velocity response spectrum by the



**DOI**: 10.1002/tal

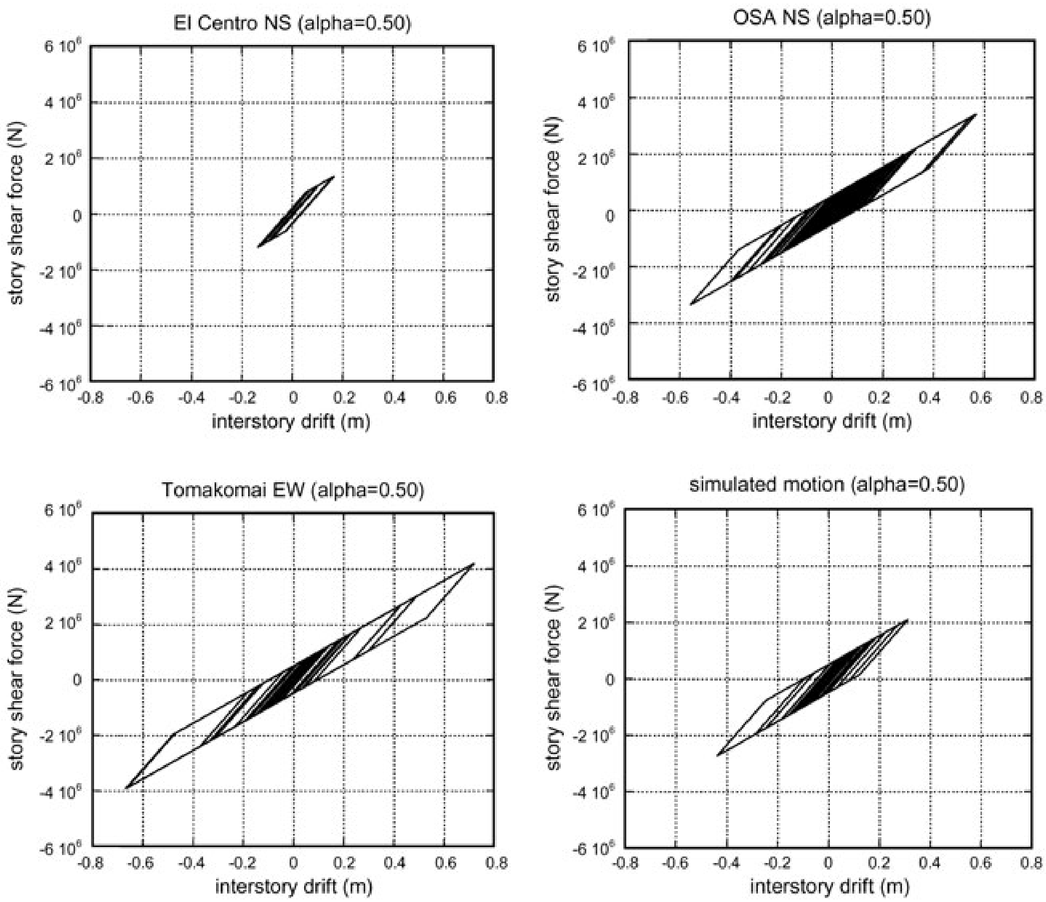


Figure 10. Restoring force characteristics in the BI system under four ground motions in the case of $\alpha = 0{\cdot}50$

natural circular frequency. For this reason, the maximum drift under Tomakomai EW in the case of $\alpha = 0{\cdot}25$ is much larger than that in the case of $\alpha = 1{\cdot}0$.

The empirical laws, known as the constant displacement law or the constant energy law (Newmark, 1970; Clough and Penzien, 1975), should be discussed from the viewpoint of the relation of the natural period of structures with the predominant period of input ground motions. Most of the recorded ground motions investigated in the proposal of such empirical laws have a predominant period smaller than 1–2 s. In such a case, structures with a fundamental natural period much larger than 1–2 s tend to follow the constant displacement law. However, those structures do not necessarily follow the constant displacement law under the long-period ground motions as shown above. The relation of the natural period of structures with the predominant period of input ground motions may be a key.

Secondly, the damping level of the additional viscous damper system in the BI system has been increased (Kelly, 1999). Figure 13 shows the corresponding figures under Tomakomai EW for the damping ratio 0·10 of the additional viscous damper system in the BI system. The maximum drifts are reduced to about 50–60% of those for the damping ratio 0·02. However, it should be remarked that this amount of damping in the additional viscous damper system in the BI system is hard to introduce and a fairly large maximum drift will be experienced in actual situations.



**DOI**: 10.1002/tal

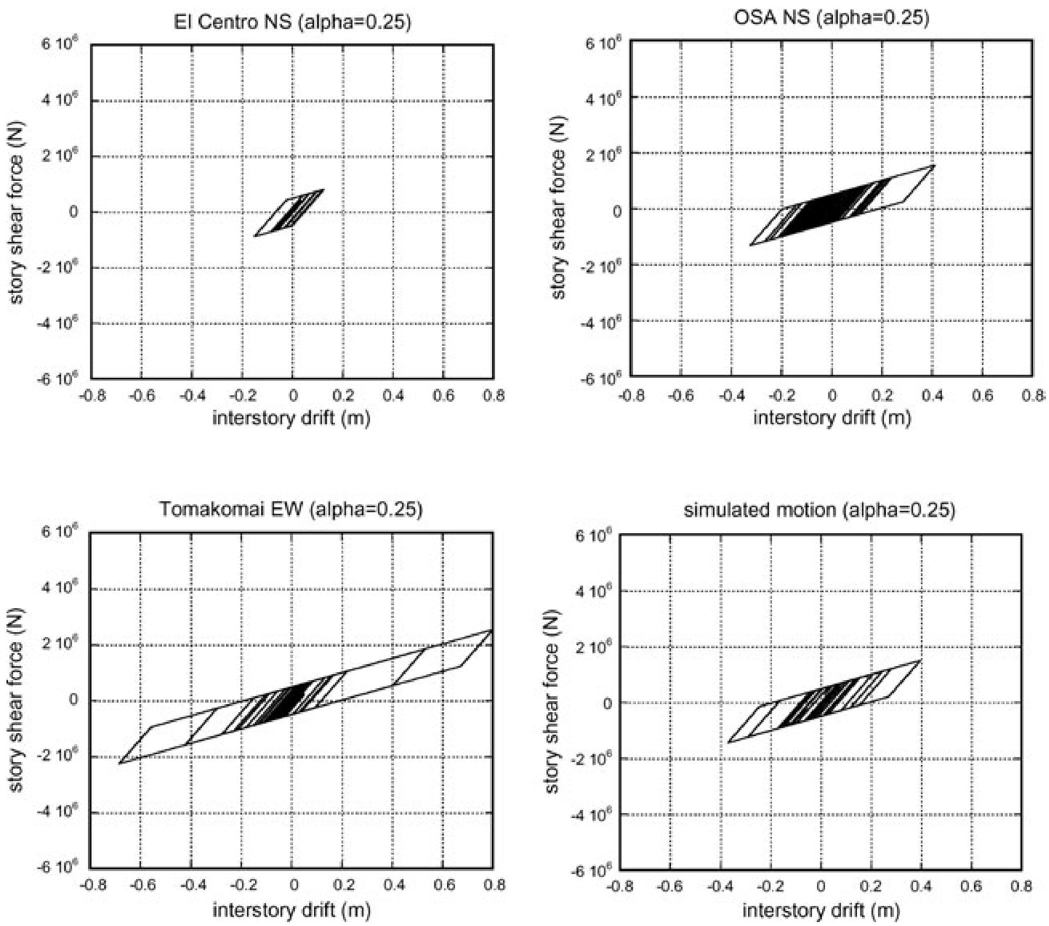


Figure 11. Restoring force characteristics in the BI system under four ground motions in the case of $\alpha = 0{\cdot}25$

Figure 14 presents the distributions of the maximum interstory drifts in the superstructure of the model with $\alpha = 0{\cdot}50$ under El Centro NS, OSA NS and Tomakomai EW for the damping ratios 0·02 and 0·10 of the additional viscous damper system in the BI system. It can be observed that, as the damping ratio increases, most of the maximum interstory drifts become smaller. However, the maximum interstory drifts in upper storeys under El Centro NS become larger in spite of the increase of the damping. This implies that special attention should be paid to the introduction of damping in the BI system.

Figure 15 shows the time histories of input energies $-\int_0^t \dot{\mathbf{u}}^T \mathbf{M1}\ddot{u}_g \mathrm{d}\tau$ (Takewaki, 2004) in four models with different parameters $\alpha = 0{\cdot}25$, 0·50, 0·75, 1·0 by Tomakomai EW. It is well known that the BI system is aimed at cutting off the energy flow into the building and it may be interesting to compare those characteristics in terms of the amount of friction-type bearings. It can be observed that, as the parameter $\alpha$ decreases, the input energy after a sufficient time decreases. However, for the parameter $\alpha$ greater than 0·50, the rate of change is small. This figure implies that, as the ratio of the friction-type bearings increases under the condition that the total initial stiffness in the BI storey is constant, the shear force in the BI storey gets smaller and the input energy decreases rapidly to a certain extent.

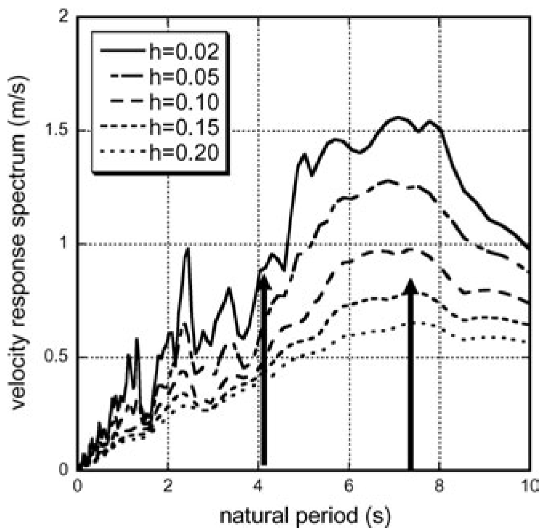


Figure 12. Velocity response spectra for various damping ratios for Tomakomai EW and the values for initial fundamental natural period (4·08 s) and equivalent fundamental natural period (7·25 s) for secant stiffness

## 4. CONCLUSIONS

The following conclusions may be drawn:

(1) BI systems with friction-type bearings are generally believed to be effective in providing damping in the BI system and avoiding resonance with ground motions by changing the equivalent natural frequency in accordance with experienced deformation. However, resonance can occur in the case where the ground motion has a large intensity of velocity response spectra with a broad band in the long natural period range. As the drift of the BI system becomes larger, resonance is accelerated because the modified natural frequency approaches the predominant period of the ground motion. This phenomenon tends not to occur in high-rise buildings without a BI system because such a drastic change of the equivalent natural frequency is unlikely to occur even in the event of minor plastic deformation in some parts.

(2) As the damping ratio of the additional viscous damper system in the BI system increases, most of the maximum interstorey drifts become smaller. However, the introduction of a sufficient amount of damping in the BI system is very difficult because of space and cost limitations. Furthermore, the maximum interstorey drifts and floor accelerations in upper storeys under some ground motions can become larger in spite of the increased damping. Therefore special attention should be paid to the introduction of damping in the BI system.

(3) The empirical laws known as constant displacement or constant energy should be discussed from the viewpoint of the relation of the natural period of structures to the predominant period of input ground motions. Over 40 years ago, most recorded ground motions had a predominant period smaller than 1–2 s. In such a case, structures with a fundamental natural period much larger than 1–2 s tend to follow the constant displacement law. However, those structures do not necessarily follow the constant displacement law under long-period ground motions. The relation of the natural period of structures with the predominant period of input ground motions is a key factor which should be carefully considered.



**DOI**: 10.1002/tal

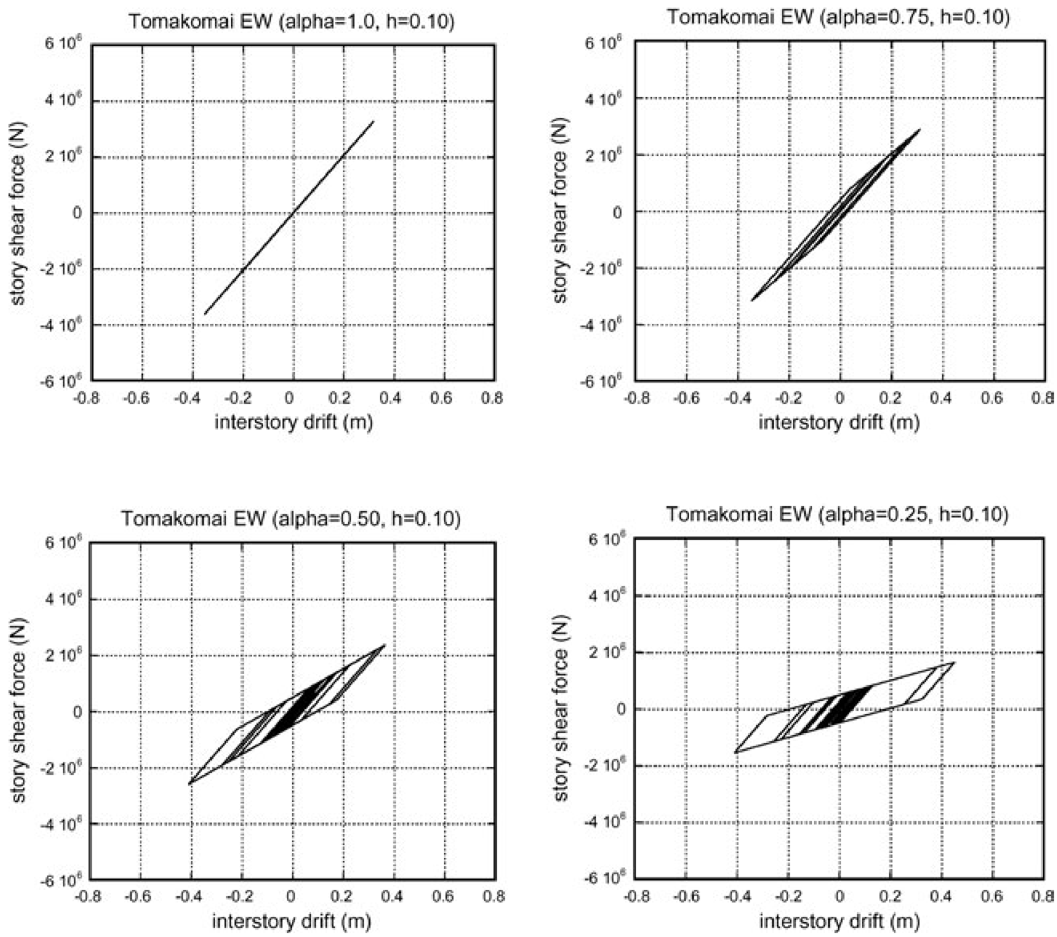


Figure 13. Restoring force characteristics in the BI system under Tomakomai EW for various $\alpha$ values for the damping ratio 0·10 of the additional viscous damper

During the Tokachi-oki earthquake on 26 September 2003, several oil tanks at Tomakomai were shaken intensively. This phenomenon was reported to result from resonance with a long-period ground motion as shown in Figures 4 and 6. The low damping level in oil tanks may be a cause of such resonant behaviour, but a similar phenomenon could occur in base-isolated buildings with rather long natural or equivalent vibration periods. These long-period ground motions were also recorded during the Kii-Hanto-Oki earthquake on 5 September 2004 and influenced the base-isolated building at Kyoto University campus (Takewaki and Nakamura, 2000; Irikura *et al*., 2004).

## ACKNOWLEDGEMENTS

Part of the present work is supported by a grant from the Kajima Foundation and a Grant-in-Aid for Scientific Research from the Japan Society for the Promotion of Science (no. 16560496). This support is greatly appreciated. The ground motions used in this paper are recorded by the Port and Airport

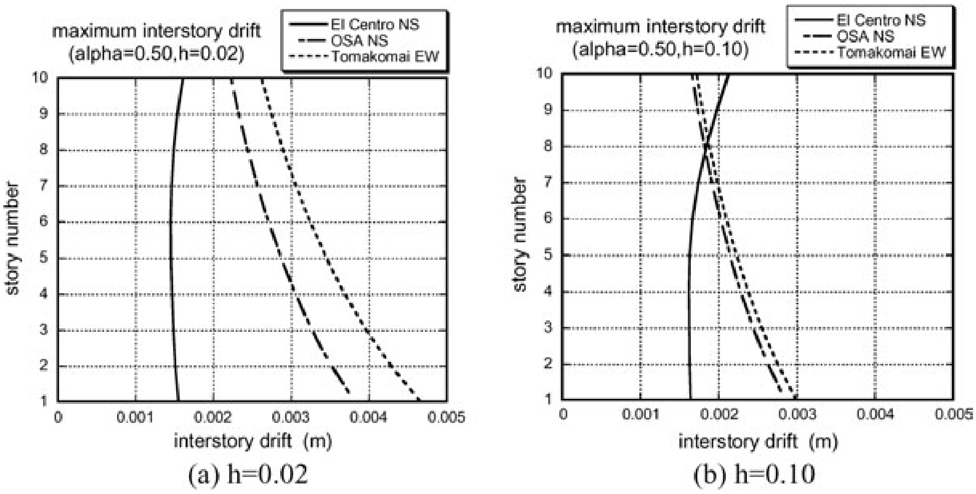


Figure 14. Maximum interstory drifts in the superstructure of the model with $\alpha = 0{\cdot}50$ under El Centro NS, OSA NS and Tomakomai EW for damping ratios 0·02 and 0·10 of the additional viscous damper

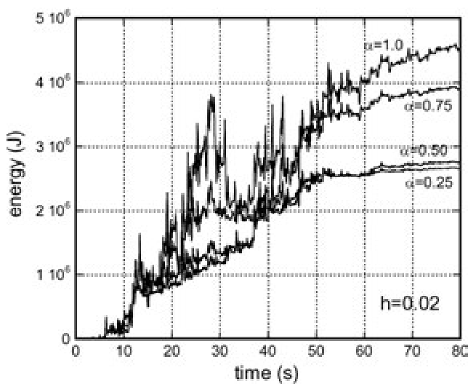


Figure 15. Time histories of input energies $-\int_0^t \dot{\boldsymbol{u}}^T \mathbf{M1}\ddot{u}_g \mathrm{d}\tau$ to four models with different parameters $\alpha = 0{\cdot}25$, 0·50, 0·75, 1·0 by Tomakomai EW

Research Institute. The simulated ground motion, denoted by OSA NS, is provided by Professors K. Irikura and K. Kamae of Kyoto University. The authors are grateful for these records and simulated motions.

## REFERENCES

Clough RW, Penzien J. 1975. *Dynamics of Structures*. McGraw-Hill: New York.

Hall JH, Heaton TH, Halling MW, Wald DJ. 1995. Near-source ground motion and its effect on flexible buildings. *Earthquake Spectra* **11**: 569–605.

Heaton TH, Hall JH, Wald DJ, Halling MW. 1995. Response of high-rise and base-isolated buildings in a hypothetical MW 7·0 Blind thrust earthquake. *Science* **267**: 206–211.



**DOI**: 10.1002/tal

Irikura K, Kamae K, Kawabe H. 2004. Importance of prediction of long-period ground motion during large earthquakes. In *Annual Conference of Seismological Society of Japan*, poster session (in Japanese).

Janjid RS, Kelly JM. 2001. Base isolation for near-fault motions. *Earthquake Engineering and Structural Dynamics* **30**: 691–707.

Kamae K, Kawabe H, Irikura K. 2004. Strong ground motion prediction for huge subduction earthquakes using a characterized source model and several simulation techniques. In *Proceedings of the 13th WCEE*, Vancouver.

Kelly JM. 1999. The role of damping in seismic isolation. *Earthquake Engineering and Structural Dynamics* **28**: 3–20.

Kobori T. 2004. *Seismic-Response-Controlled Structure* (new edn). Kajima: Tokyo.

Naeim F, Kelly JM. 1999. *Design of Seismic Isolated Structures.* Wiley: New York.

Nakamura T, Yamane T. 1986. Optimum design and earthquake-response constrained design for elastic shear buildings, *Earthquake Engineering and Structural Dynamics* **14**: 797–815.

Newmark NM. 1970. Current trends in the seismic analysis and design of high-rise structures. In *Earthquake Engineering* Wiegel RL (ed.) Prentice-Hall: Englewood Cliff., NJ: Ch. 16.

Takewaki I. 2004. Bound of earthquake input energy. *Journal of Structural Engineering ASCE* **130**(9): 1289–1297.

Takewaki I, Nakamura M. 2000. Stiffness–damping simultaneous identification using limited earthquake records. *Earthquake Engineering and Structural Dynamics* **29**(8): 1219–1238.



**DOI**: 10.1002/tal